Optical textures: characterizing spatiotemporal chaos

MARCEL G. CLERC,[1] **GREGORIO GONZÁLEZ-CORTÉS,**[1] **VINCENT ODENT,**[1,2] **AND MARIO WILSON** [1,3,*]

[1]*Departamento de Física, Facultad de Ciencias Físicas y Matemáticas, Universidad de Chile, Blanco Encalada 2008, Santiago, Chile*

[2]*Present address: Université Lille 1, Laboratoire de Physique des Lasers, Atomes et Molécules, CNRS UMR8523, 59655 Villeneuve d'Ascq Cedex, France*

[3]*CONACYT – CICESE, Carretera Ensenada-Tijuana 3918, Zona Playitas, C.P. 22860, Ensenada, Mexico*

[*]*mwilson@cicese.mx*

Abstract: Macroscopic systems subjected to injection and dissipation of energy can exhibit complex spatiotemporal behaviors as result of dissipative self-organization. Here, we report a one- and two-dimensional pattern forming setup, which exhibits a transition from stationary patterns to spatiotemporal chaotic textures, based on a nematic liquid crystal layer with spatially modulated input beam and optical feedback. Using an adequate projection of spatiotemporal diagrams, we determine the largest Lyapunov exponent. Jointly, this exponent and Fourier transform allow us to distinguish between spatiotemporal chaos and amplitude turbulence concepts, which are usually merged.

References and links

1. F. T. Arecchi, G. Giacomelli, P. L. Ramazza, and S. Residori, "Experimental evidence of chaotic itinerancy and spatiotemporal chaos in optics," Phys. Rev. Lett. **65**, 2531–2534 (1990).
2. G. Huyet, M. C. Martinoni, J. Tredicce, and S. Rica, "Spatiotemporal dynamics of lasers with a large Fresnel number," Phys. Rev. Lett. **75**, 4027–4030 (1995).
3. G. Huyet and J. R. Tredicce, "Spatio-temporal chaos in the transverse section of lasers," Physica D **96**, 209–214 (1996).
4. A. V. Mamaev and M. Saffman, "Selection of unstable patterns and control of optical turbulence by Fourier plane filtering," Phys. Rev. Lett. **80**, 3499–3502 (1998).
5. E. A. Rogers, R. Kalra, R. D. Schroll, A. Uchida, D. P. Lathrop, and R. Roy, "Generalized synchronization of spatiotemporal chaos in a liquid crystal spatial light modulator," Phys. Rev. Lett. **93**, 084101 (2004).
6. S. Residori, "Patterns, fronts and structures in a liquid-crystal-light-valve with optical feedback," Phys. Rep. **416**, 201–272 (2005).
7. K. Staliunas and J. Sánchez-Morcillo, *Transverse Patterns* (Springer Science & Business Media, 2003).
8. O. Descalzi, M. G. Clerc, S. Residori, and G. Assanto, eds., *Localized States in Physics: Solitons and Patterns* (Springer Science & Business Media, 2011).
9. M. Tlidi, K. Staliunas, K. Panajotov, A. G. Vladimirov, and M. G. Clerc, "Localized structures in dissipative media: from optics to plant ecology," Phil. Trans. R. Soc. A **372**, 20140101 (2014).
10. G. Nicolis and I. Prigogine, *Self-Organization in Non Equilibrium Systems* (J. Wiley & Sons, 1977).
11. G. Nicolis, *Introduction to Nonlinear Science* (Cambridge University, 1995).
12. P. Coullet and J. Lega, "Defect-mediated turbulence in wave patterns," Europhys. Lett. **7**, 511–516 (1988).
13. P. Coullet, L. Gil, and J. Lega, "Defect-mediated turbulence," Phys. Rev. Lett. **62**, 1619–1622 (1989).
14. G. Goren, J. P. Eckmann, and I. Procaccia, "Scenario for the onset of space-time chaos," Phys. Rev. E **57**, 4106–4134 (1998).
15. W. Decker, W. Pesch, and A. Weber, "Spiral defect chaos in Rayleigh-Benard convection," Phys. Rev. Lett. **73**, 648–651 (1994).
16. B. Echebarria and H. Riecke, "Defect chaos of oscillating hexagons in rotating convection," Phys. Rev. Lett. **84**, 4838–4841 (2000).
17. K. E. Daniels and E. Bodenschatz, "Defect turbulence in inclined layer convection," Phys. Rev. Lett. **88**, 034501 (2002).
18. M. Miranda and J. Burguete, "Experimentally observed route to spatiotemporal chaos in an extended one-dimensional array of convective oscillators," Phys. Rev. E **79**, 046201 (2009).

19. P. Brunet and I. Limat, "Defects and spatiotemporal disorder in a pattern of falling liquid columns," Phys. Rev. E **70**, 046207 (2004).
20. Q. Ouyang and J. M. Flesselles, "Transition from spirals to defect turbulence driven by a convective instability," Nature **379**, 143–146 (1996).
21. A. Garfinkel, M. L. Spano, W. L. Ditto, and J. N. Weiss, "Controlling cardiac chaos," Science **257**, 1230–1235 (1992).
22. S. Q. Zhou and G. Ahlers, "Spatiotemporal chaos in electroconvection of a homeotropically aligned nematic liquid crystal," Phys. Rev. E **74**, 046212 (2006).
23. S. J. Moon, M. D. Shattuck, C. Bizon, D. I. Goldman, J. B. Swift, and H. L. Swinney, "Phase bubbles and spatiotemporal chaos in granular patterns," Phys. Rev. E **65**, 011301 (2001).
24. N. Verschueren, U. Bortolozzo, M. G. Clerc, and S. Residori, "Spatiotemporal chaotic localized state in liquid crystal light valve experiments with optical feedback," Phys. Rev. Lett. **110**, 104101 (2013).
25. N. Verschueren, U. Bortolozzo, M. G. Clerc, and S. Residori, "Chaoticon: localized pattern with permanent dynamics," Phil. Trans. R. Soc. A. **372**, 20140011 (2014).
26. P. Manneville, *Dissipative Structures and Weak Turbulence* (Academic, 1990).
27. L. Pastur, U. Bortolozzo, and P. L. Ramazza, "Transition to space-time chaos in an optical loop with translational transport," Phys. Rev. E **69**, 016210 (2004).
28. M. G. Clerc, G. Gonzalez-Cortes, and M. Wilson, "Experimental Spatiotemporal Chaotic Textures in a Liquid Crystal Light Valve with Optical Feedback," in *Nonlinear Dynamics: Materials, Theory and Experiments*, M. Tlidi and M. G. Clerc, eds. (Springer, 2016).
29. M. G. Clerc, C. Falcon, M. A. Garcia-Nustes, V. Odent, and I. Ortega, "Emergence of spatiotemporal dislocation chains in drifting patterns," Chaos **24**, 023133 (2014).
30. E. Louvergneaux, "Pattern-Dislocation-Type Dynamical Instability in 1D Optical Feedback Kerr Media with Gaussian Transverse Pumping," Phys. Rev. Lett. **87**, 244501 (2001).
31. S. Bielawski, C. Szwaj, C. Bruni, D. Garzella, G. L. Orlandi, and M. E. Couprie, "Advection-induced spectrotemporal defects in a free-electron laser" Phys. Rev. Lett. **95**, 034801 (2005).
32. G. Nicolis, *Introduction to Nonlinear Science* (Cambridge University, 1995).
33. M. G. Clerc and N. Verschueren, "Quasiperiodicity route to spatiotemporal chaos in one-dimensional pattern-forming systems," Phys. Rev. E. **88**, 052916 (2013).
34. K. E. Daniels and E. Bodenschatz, "Defect turbulence in inclined layer convection," Phys. Rev. Lett. **88**, 034501 (2002).
35. Y. Kuramoto, *Chemical Oscillations: Waves, and Turbulence* (Springer, 1984).
36. U. Frisch, *Turbulence: the Legacy of A.N. Kolmogorov* (Cambridge University, 1995).
37. A. Wolf, J. B. Swift, H. L. Swinney, and J. A. Vastano, "Determining the Lyapunov exponents from a time series," Physica D **16**, 285–317 (1985).
38. E. Ott, *Chaos in Dynamical Systems*, 2nd ed. (Cambridge University, 2002).
39. H. Abarbanel, *Analysis of Observed Chaotic Data* (Springer-Verlag, 1996).

1. Introduction

Optical systems maintained far from equilibrium, through the injection and dissipation of energy, can present spatiotemporal structures, *patterns* [1–9]. These structures appear as a way to optimize energy transport and momenta [10]. Patterns are the result of the interplay between the linear gain and the nonlinear saturation mechanisms. In many physical systems, these structures are stationary and emerge as a spatial instability of a uniform state when a control parameter is changed and surpasses a critical value, which usually corresponds to imbalances of forces. As the parameters of the system are changed, stationary patterns can become unstable and bifurcate to more complex patterns, even into aperiodic dynamics states [11–14]. This behavior is characterized by complex spatiotemporal dynamics exhibited by the pattern and a continuous coupling between spatial modes in time. Complex spatiotemporal dynamics of patterns have been observed, for example, in fluids [15–19], chemical reaction-diffusion systems [20], cardiac fibrillation [21], electroconvection [22], fluidized granular matter [23], nonlinear optical cavities [1–4] and in a liquid crystal light valve [6, 24, 25]. In most of these studies, complex behaviors are characterized by spatial and temporal Fourier transforms, wave vector distribution, filtering spatiotemporal diagrams, power spectrum of spatial mode, length distributions, Poincaré maps and number of defects as a function of the parameters. However, in these experimental studies, spatiotemporal complexity has not been characterized using rigorous tools of dynamical systems theory as Lyapunov exponents [26, 27]. These exponents
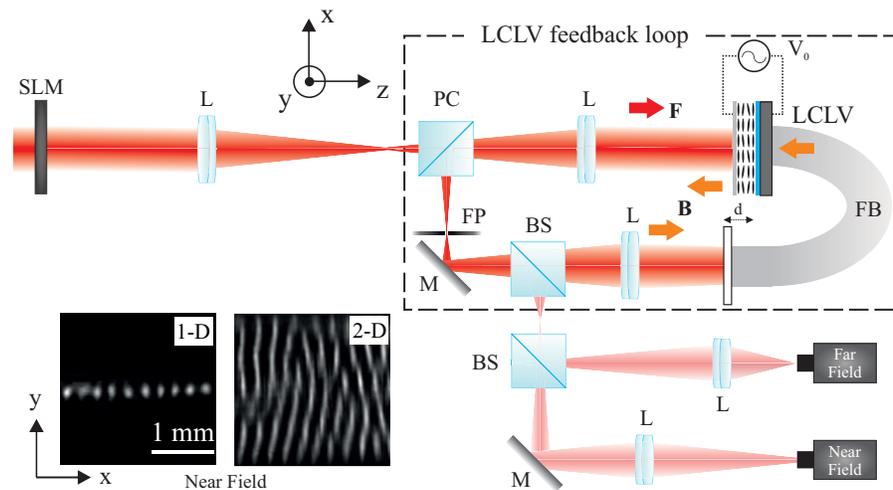
Fig. 1. Schematic representation of the experimental setup. LCLV stands for the liquid crystal light valve, L represents the achromatic lenses with a focal distance $f = 25\,cm$, M are the mirrors, FB is an optical fiber bundle, BS stands for the beam splitters, PC represents a polarizing cube, SLM is a spatial light modulator and FP represents the Fourier plane. F and B stand for the forward (incoming) and backward (reflected) beam respectively. d is the equivalent optical length. In the bottom left part of the image, two examples of obtained patterns and textures.

characterize the exponential sensitivity of the dynamical behaviors under study and in turn gives a characteristic time scale on which one has the ability to predict the time evolution of the system. When the largest Lyapunov exponent (LLE) is positive (negative) the system under study is chaotic (stationary). Recently, we have computed the experimental LLE and characterized the spatiotemporal chaos in two spatial dimensions in a liquid crystal light valve (LCLV) with optical feedback [28]. The dynamics exhibited by the LCLV with optical feedback is characterized by the changes that molecular orientation induces in the phase of the reflected light, which, in its turn—optical feedback—produces a voltage that reorients the liquid crystal molecules.

One of the most important concepts in complex spatiotemporal dynamics is turbulence: the power spectrum as a result of the transport of some physical quantity of different scales shows a power law decay as its main signature [36]. The aim of this article is to investigate one and two dimensional pattern forming system in a LCLV, shown in Fig. 1, which exhibits a transition from stationary patterns to spatiotemporal chaotic textures and to quasiperiodicity. Using adequate spatiotemporal diagrams, we obtain the LLE. Jointly, this exponent and Fourier transform allow us to distinguish between spatiotemporal chaos and amplitude turbulence concepts, which are usually merged.

2. Experimental details

The liquid crystal light valve with an optical feedback is a flexible optical experimental setup that exhibits pattern formation [6] [see Fig. 1]. The LCLV is illuminated by an expanded and collimated He-Ne laser beam, $\lambda = 633\,nm$, with 3 cm transverse diameter and power $I_{in} = 6.5$ mW/cm^2, linearly polarized along the vertical axis. Once shone into the LCLV, the beam is reflected by the dielectric mirror deposed on the rear part of the cell and, thus, sent to the polarizing cube. Due to the phase-change the light suffers in the reflection, the polarizing cube will send the reflected light into the feedback loop. To close the feedback loop, a mirror and an optical fiber bundle are used, these elements assure the light to reach the photoconductor

placed in the back part of the LCLV. In the feedback loop, a 4-f array is placed in order to obtain a self-imaging configuration and access to the Fourier plane, this array is constructed with 2 identical lenses with focal length $f = 25\ cm$ placed in such a way that both sides of the LCLV are conjugated planes. We filter the Fourier plane in order to force the system to exhibit roll-patterns in a given direction. Thanks to this configuration the free propagation length in the feedback loop can be easily adjusted. For the performed experiments an optical equivalent length of $d = -4$ cm was used. A spatial light modulator (SLM) was placed in the input beam optical path with a $1:1$ imaging between the SLM and the frontal part of the LCLV. With the aid of a specialized software, a square mask was produced and sent to the SLM. The SLM and the polarizing cube combination allow to impose an arbitrary shape to the input beam. For a uniform mask of 160 gray-value, the typical input intensity would be $I_w = 0.83\ mW/cm^2$. To obtain the shape used in the experiments, one and two-dimensional masks, $I(x,y)$, were created and, by means of these masks, one and two dimensional patterns can be obtained as can be seen in the bottom left part of Fig. 1. The system dynamics is controlled by adjusting the external voltage V_0 applied to the LCLV.

3. From stationary to disordered dynamics

The presented dynamics in the LCLV have been explored in two different configurations, the first one using an intensity mask of zero-level intensity everywhere except for a central square part with length $a_0 = 2.5$ mm (2-D mask), and the second one with a zero-level intensity except on a narrow channel of 150 μm width and 2.5 mm length (1-D mask). The injected intensity is spatially modulated as $I_{in} = I_0(x,y)$, where I_0 can be controlled by changing the mask created in the SLM, and $\{x,y\}$ are the transverse coordinates of the sample. I_0 is measured when imposing a given gray-value to the illuminated area, that is, for the 2-D mask

$$I_0(x,y) = \begin{cases} I_0 + b_0 & |x| \le a_0, \text{ and } |y| \le a_0 \\ b_0 & else \end{cases}$$

when b_0 is constant throughout the sample and $|x| > 0$, $|y| > 0$. The same applies to 1-D mask with the only difference that $|y| = 150\ \mu$m, which is small enough, compared with the pattern wavelength, to neglect its size and consider it as a 1-D mask. In the presented configurations $I_0 = 0.9\ mW/cm^2$ and $b_0 = 0.1\ mW/cm^2$. The alternating voltage V_0 has been varied between 3 and 7 V_{rms}, at a constant frequency $f_0 = 5\ kHz$, starting with the appearance of stationary roll-patterns. For different V_0 values, the dynamical behavior obtained in the system was recorded with a CCD camera. Figure 2 shows the spatiotemporal evolution of the observed patterns in one and two dimensions, respectively. This evolution is characterized by projected spatiotemporal diagrams, which are constructed, in the 2-D experiments, by picking an arbitrary line—transversal to the rolls direction—in the illuminated zone and superposing it as time evolves; in the 1-D experiments this construction is simpler, is enough to superpose the pattern as the time evolves. The system exhibits stationary stripe patterns [cf. Fig. 2(a)]. These patterns are induced by a spatial filtering in the Fourier plane [cf. FP in Fig. 1]. Actually, through a slit, we can filter spatial modes.

Increasing V_0, the dynamics shown by the pattern becomes abruptly complex [cf. Figs. 2(b) and 2(d)]. Clearly, in the projected spatiotemporal diagram, we detected an intermittent behavior. That is, the pattern exhibits aperiodic oscillations invaded by large fluctuations, generating several spatial and temporal dislocations. Likewise, the system exhibits a high spatiotemporal complexity. This kind of disorder is usually associated to spatiotemporal chaotic textures [28, 32–34]. Figure 2(d) shows a 3-D spatiotemporal diagram, from this diagram it is clear that an arbitrarily chosen line represents the dynamics.

Further increasing V_0, the pattern begins to oscillate in a complex manner [see Fig. 2(c)]. We observe in the projected spatiotemporal diagram local waves, oscillations and spatiotemporal
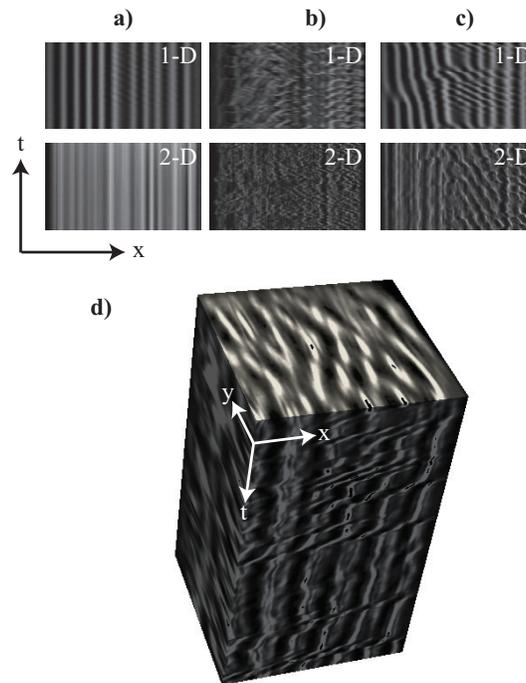
Fig. 2. Spatial textures in LCLV with optical feedback at different voltage V_0. Top panels correspond to spatiotemporal diagrams of observed dynamics working with one-dimensional patterns. Middle panels panels stand for projected spatiotemporal diagrams of two-dimensional textures. a) Periodic regime, b) chaotic behavior, c) quasi-periodic dynamics, and d) a 3-D spatiotemporal diagram of a complex texture found in the intermittent regime at $V_0 = 4.3V\,rms$. All values were taken during $100\,s$ and are normalized.

dislocations. Similar dynamics has been reported in one-dimensional inhomogeneous systems [29–31]. In our experiments these inhomogeneities can be caused by the inherent imperfections and inhomogeneities induced by the filter in the Fourier plane. Hence, this kind of dynamical behavior could be expected. The complex dynamics exhibited by this pattern is constantly repeated over time. Which leads us to infer that this kind of behavior could be quasiperiodicity.

A mathematical tool for analyze the spatial modes interaction is the Fourier spectrum. Figure 3 shows the Fourier spectra of different dynamical regimes. Showing that the dynamics changes between stripe patterns, quasi-periodicity and spatiotemporal chaotic textures. The stationary pattern is characterized by a dominant wavelength f. The width of this peak is due to temperature fluctuations and dynamics of defects such as dislocations and boundary grains. The quasi periodic texture is characterized by the appearance of incommensurable wavelengths, $\{f', f'''\}$, with respect to the main wavelength f'' and its harmonics. The spatiotemporal chaotic texture is characterized by presenting an enlarged spectrum as a result of the interaction between the main incommensurable modes [35]. Note that in this regime, the modes are coupled with exponential decay [see the dashed line in Fig. 3]. Therefore, the system does not exhibit power spectrum behavior which is the hallmark of turbulence dynamics [36].

4.   Quantifying the dynamics

A characterization of complex dynamics like chaos and spatiotemporal chaos can be done by means of Lyapunov exponents. There are as many exponents as the dimension of the system
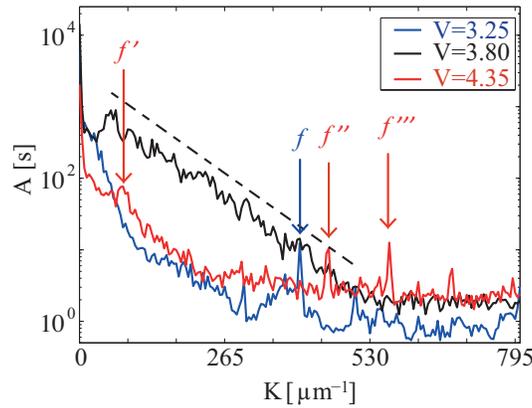
Fig. 3. Fourier spectra for three different dynamical regimes. In gray (blue) the Fourier spectrum of a stationary pattern, in light-gray (red) a quasi-periodic regime, it can be observed the emergence of incommensurable frequencies (f', f'' and f'''). In black, a broadened spectrum that corresponds to a chaotic texture, presenting an exponential decay of the modes marked by the dashed line.

under study. The analytical study of Lyapunov exponents is a paramount endeavor and in practice inaccessible, then the pragmatic strategy is a numerical derivation of the exponents. From experimental data, in the case of low-dimensional dynamical systems, by means of recognition of initial conditions one can determine the LLE [37]. This exponent accounts for the greatest exponential growth and its defined by

$$\lambda_0 = \lim_{t \to \infty} \lim_{\Delta_0 \to 0} \frac{1}{t} \ln \left[\frac{||\mathbf{u}(x,t) - \mathbf{u}'(x,t)||}{||\mathbf{u}(x,t_o) - \mathbf{u}'(x,t_o)||} \right], \tag{1}$$

where $\mathbf{u}(x,t)$ and $\mathbf{u}'(x,t)$ are given fields, $\Delta_o \equiv ||\mathbf{u}(x,t_0) - \mathbf{u}'(x,t_0)||$ and $||f(x,t)||^2 \equiv \int |f(x,t)|^2 dx$ is a norm. $\Delta(t) \equiv ||\mathbf{u}(x,t) - \mathbf{u}'(x,t)||$ stands for the global evolution of the difference between the fields.

When λ_0 is positive or negative, the perturbation of a given trajectory is characterized by an exponential separation or approach, respectively. Dynamical behaviors with zero LLEs correspond to equilibrium with invariant directions, such as periodic or quasi-periodic solutions and non-chaotic attractors [38]. Hence, the LLE is an exceptional order parameter for characterizing transitions from stationary to complex spatiotemporal dynamics.

Experimentally, to estimate the LLE, it is mandatory to have two close initial conditions and observe if their evolution diverge at large times [28]. The implemented method needs, as a first step, to find two close fields [see lines 1 and 2 in Figs. 4(a) and 4(b)] along the projected spatiotemporal diagrams and compute their difference Δ_0. The temporal evolution of the difference should be given by $\Delta(t) \approx \Delta_0 e^{\lambda_0 t}$ for large t [cf Figs. 4(c) and 4(d)]. Due to the complexity of evolution of the difference between fields—clearly the number of positive Lyapunov exponents is huge—we will consider at least two unstable growth directions, that is $\Delta(t) \approx a e^{bt} + c e^{dt}$ [cf. Fig. 4].

A bifurcation diagram was constructed with the obtained LLEs as can be seen in Fig. 5. The system starts with stationary stripe patterns at $V_0 = 3.0\,V_{rms}$ and the dynamics remains unchanged until the applied voltage reached $V_0 = 3.5\,V_{rms}$. At this voltage, the LLE goes to zero, meaning that the system exhibits a bifurcation. Experimentally, we observed that the steady pattern changes to an aperiodic regime. The chaotic behavior remains until the mean intensity in the LCLV destroys the chaotic attractor due to destructive interference at $V_0 = 3.9\,V_{rms}$ [see
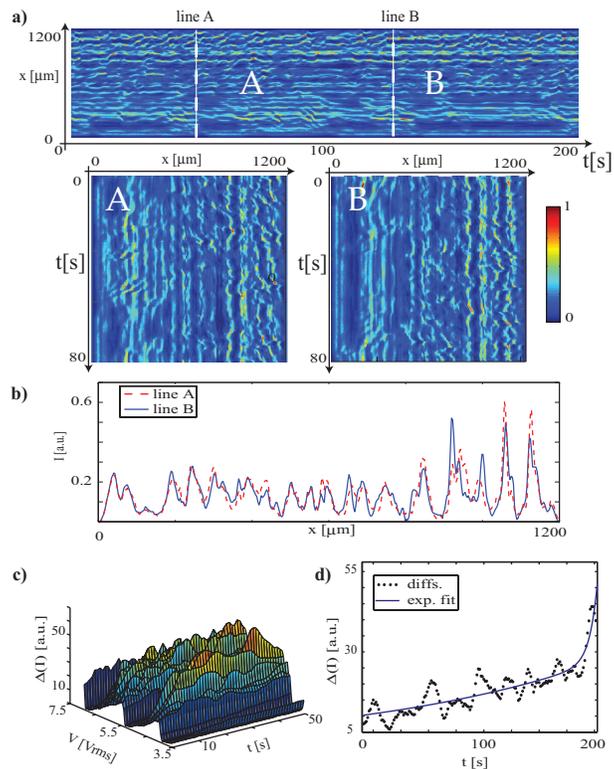
Fig. 4. LLE estimation for the LCLV with optical feedback with $V_0 = 4.70 V_{rms}$. a) Projected spatiotemporal diagram of the LCLV. The bottom panels account for spatiotemporal diagram with close initial conditions (lines 1 and 2), b) Intensity profiles of lines 1 and 2, c) A 3-D graph that shows evolution of differences $\Delta(t, V_0)$ for different applied voltages V_0, it can be noted that not always the trajectories are exponentially separated, and d) Temporal evolution of global difference $\Delta(t)$, dots stand for experimental data and the continuous curve is the exponential fitting $\Delta(t) \approx a e^{bt} + c e^{dt}$ with $a = 0.0045$, $b = 8.813$, $c = 16.57$ and $d = 0.2773$.
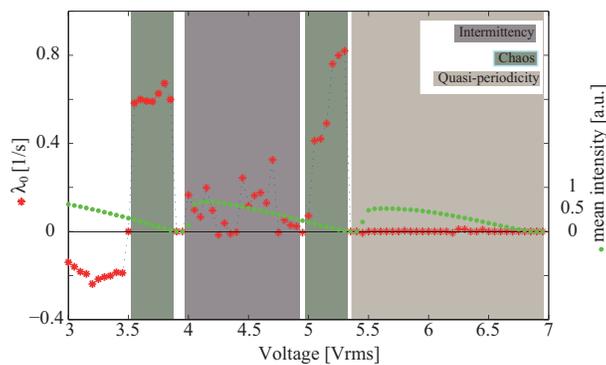

Fig. 5. Bifurcation diagram constructed with the estimated LLE as a function of applied voltage V_0 of the LCLV with optical feedback. The diagram is clearly separated in four dynamical regimes, stationary patters before $V_0 = 3.5 V_{rms}$, chaos shadowed in gray (green), intermittency between chaos and quasi-periodicity in dark gray (gray) area and a window of quasi-periodicity shadowed at the end in light gray. The stars correspond to the calculated LLE while the circles show the normalized mean intensity present in the LCLV.

Fig. 5], causing a crisis. Once the light is recovered, the system enters in an intermittent regime between chaos and quasi-periodicity. After this window the system becomes chaotic until the attractor is annihilated by destructive interference at $V_0 = 5.35\,V_{rms}$. Once the light is recovered the system remains in a quasi-periodic regime until the next cycle of destructive interference arrives. This dynamic regime is characterized by having an oscillatory pattern which LLE is zero.

Given a temporal signal, the attractor of the system can be built by taking the signal at different periodic times (arbitrary periodic separation τ) and constructing the vector $\{I(x,t), I(x,t + \tau,x), I(x,t+2\tau), \cdots\}$ with x as a fixed position, *phase space reconstruction* [39]. The three different attractors that can be reconstructed using this embedding method are a fixed point, a torus and a strange attractor. For low voltage a fixed point can be seen (stationary pattern). Increasing the tension V_0, the phase space reconstruction exhibits a torus (quasi-periodic pattern) and strange attractor (spatiotemporal texture) [28].

5. Conclusions

Our study provides clear evidence that the LCLV with optical feedback is spatiotemporally chaotic in a certain range of parameters. The LLEs are experimentally accessible and allow us to characterize the transitions from stationary to complex spatiotemporal dynamics. Certainly new concepts in the theory of dynamical systems must be developed to achieve a better experimental characterization of spatiotemporal complex behaviors. Notwithstanding, jointly the LLEs and power spectrum allow us distinguishing well-established dynamical behaviors such as amplitude turbulence and spatiotemporal chaos, which are often merged and confused.

Acknowledgments